Scientific paper

Theoretical Studies on Stabilities and Spectroscopy of $C_{80}CH_2$

Xuguang Wen[a], Xin Ren[b] and Shi Wu[a,*]

[a] *Department of Chemistry, Zhejiang University, Hangzhou 310027, China*

[b] *Department of Pharmacy, Zhejiang University, Hangzhou 310027, China*

** Corresponding author: E-mail: wushi@zju.edu.cn*
tel: 8657188206529; fax: 8657188206529

Received: 29-02-2008

Abstract

The electronic structures and stabilities of the nine possible isomers of $C_{80}CH_2$ based on $C_{80}(D_{5d})$ were studied using density function theory (DFT) at B3LYP/6-31G level. Based on the optimized geometries, the electronic spectra, IR and ^{13}C NMR spectra of the isomers of $C_{80}CH_2$ were calculated using INDO/CIS, PM3 and B3LYP/6-31G methods, respectively. The most stable geometry of $C_{80}CH_2$ is predicted to be 27,28–$C_{80}CH_2$(A) with an annulene structure, where the additive bond is 6/6 bond near the equatorial belt of $C_{80}(D_{5d})$. Compared with those of $C_{80}(D_{5d})$, the first absorptions in the electronic spectra and main absorptions in the IR spectra of the stable $C_{80}CH_2$ isomers are red-shifted. The ^{13}C chemical shifts of the bridged carbon atoms in the cyclopropane structures in comparison with those in the annulene structures are changed upfield. The aromaticities are better maintained in the annulene structures than cyclopropane structures according to the NICS values of $C_{80}CH_2$ at B3LYP/6-31G level.

Keywords: $C_{80}CH_2$, B3LYP/6-31G, electronic spectra, ^{13}C NMR, NICS.

1. Introduction

The functionalization of fullerenes has been an interesting research topic for scientists. One of the C_{80} isomers with D_{5d} symmetry has been successfully isolated and characterized with ^{13}C NMR and UV spectra. The ^{13}C NMR results suggested that there are five types of carbon atoms in $C_{80}(D_{5d})$.[1] The energy gap of $C_{80}(D_{5d})$ calculated using AM1 method is 4.72 eV.[2] $C_{80}(D_{5d})$ has been found to be the lowest-energy isomer with the wide energy gap at HF/4-31G level.[3] The optical gap of C_{80} is reduced and the UV-vis-NIR absorption is red-shifted owing to the addition of the two CF_3 groups.[4] Many exohedral adducts of C_{80} like $Sc_3N@C_{80}(CH_2)_2NR$ and n-$Bu_4N^+[Sc_3C_2@C_{80}(Ad)]^-$ have been synthesized with the help of the high stabilities improved by endohedral complexes containing metal or other groups.[5,6] On one hand, the reactivity of C_{80} can be improved due to the dense negative charge on the surface caused by the electronic transfer from the inside metals to the fullerene cage.[5] On the other hand, the X-ray determination can be easily performed because of the cycloaddition of the adamantylidene carbene (Ad) to the cage.[6] The methylene adducts of C_{60} and C_{70} can be prepared by direct carbene addition and dipolar cycloadditions of diazo compounds.[7] Similar covalent derivatives of C_{78} have been obtained through the reaction between fullerenes and diethyl 2-bromomalonate.[8] These derivatives like T_h–$C_{60}(C(COOH)_2)_6$ can be used as electrolytes.[9] Hitherto, the methylene adducts of $C_{80}(D_{5d})$ have not been synthesized.

Although $C_{80}O$ has been studied theoretically,[10,11] $C_{80}CH_2$ based on $C_{80}(D_{5d})$ has not been investigated yet. Herein the nine possible geometries of $C_{80}CH_2$ are explored to predict the properties of $C_{80}CH_2$ and simulate similar derivatives. First, we want to know which geometry of $C_{80}CH_2$ is the most stable one and whether the additive bond is opened. Then we want to study the electronic structures and spectroscopy of $C_{80}CH_2$. Finally, we want to study the aromaticity of $C_{80}CH_2$ through computing the NICS values.

2. Research Approach

An initial geometry of $C_{80}(D_{5d})$ was drawn in Chem3D, and the full geometry optimization without any

symmetric restriction was performed using PM3 method and DFT at B3LYP/STO-3G, B3LYP/3-21G and B3LYP/6-31G levels progressively in Gaussian 03 program package.[12] These methods have been used to study the electronic structures and stabilities of the supramolecular complexes,[13] conducting polymers,[14] and other organic compounds.[15] Then the equilibrium geometry of $C_{80}(D_{5d})$ was obtained. There are 5 unique carbon atoms and nine kinds of C–C bonds in $C_{80}(D_{5d})$. Based on the optimized geometry of $C_{80}(D_{5d})$ at B3LYP/6-31G level, CH_2 was added to the nine different bonds above the equatorial belt of $C_{80}(D_{5d})$, respectively. In the isomer 27,28–$C_{80}CH_2$(A) (Figure 1), 27,28- stands for the bond added by CH_2. This numbering system was according to the IUPAC rule for carbon clusters.[16] These isomers of $C_{80}CH_2$ were optimized in the same way as the above, then the equilibrium geometries with the minimum energy of $C_{80}CH_2$ were accomplished. According to Koopmans' theory, vertical ionization potential (IP) is approximately defined as the negative value of HOMO (the highest occupied molecular orbital) energy. Vertical electron affinity (EA) is defined as the negative value of LUMO (the lowest unoccupied molecular orbital) energy. Absolute hardness (η) is equal to the half of the difference between IP and EA. Absolute electron negativity (χ) is defined as the half of the sum for IP and EA. All these variables were calculated at B3LYP/6-31G level.

Based on the B3LYP/6-31G optimized geometries of $C_{80}CH_2$, the electronic spectra were computed using INDO/CIS method[17] without any adjustment of the parameters.[18] One hundred and ninety-seven configurations including the ground state were generated by exciting electrons from 14 HOMOs to 14 LUMOs. The IR spectra were calculated using PM3 method. The ^{13}C NMR spectra and NICS (nucleus independent chemical shifts) values of the isomers were calculated on GIAO (gauge-including atomic orbitals) method at B3LYP/6-31G level. The NICS values were used to measure the aromaticity, which was proposed by Schleyer *et al.*[19]

3. Results and Discussion

Relative energies at B3LYP/6-31G level: The optimized results of $C_{80}(D_{5d})$ were compared with the experimental values and other calculation results to assure the reliability of the method. The bond lengths of $C_{80}(D_{5d})$ at B3LYP/6-31G level are within the range of 0.1395–0.1473 nm, which is consistent with the ranges of 0.1391–0.1462 and 0.140–0.146 nm calculated using ZINDO and SCF-MO methods.[20,21] The length and width in the polar and equatorial directions of $C_{80}(D_{5d})$ are 0.9169 and 0.6773 nm, which are in agreement with the calculated results (0.946 and 0.716 nm).[21] The ratio between the long and short axes of $C_{80}(D_{5d})$ is 1.35, which is compatible with the experimental value 1.3.[1]

According to the relative energies of $C_{80}CH_2$ isomers (Table 1), the most stable geometry of $C_{80}CH_2$ is found to be 27,28–$C_{80}CH_2$(A), where the CH_2 group is added to the C(27)–C(28) bond near the equatorial belt of $C_{80}(D_{5d})$ (Figure 1). The length 0.1468 nm of the C(27)–C(28) bond is relatively larger than the others in $C_{80}(D_{5d})$ since the C(27)–C(28) bond is surrounded by four neighbored hexagons. Thus the C(27)–C(28) bond is weak and easy to undergo an addition. The second stable isomer is

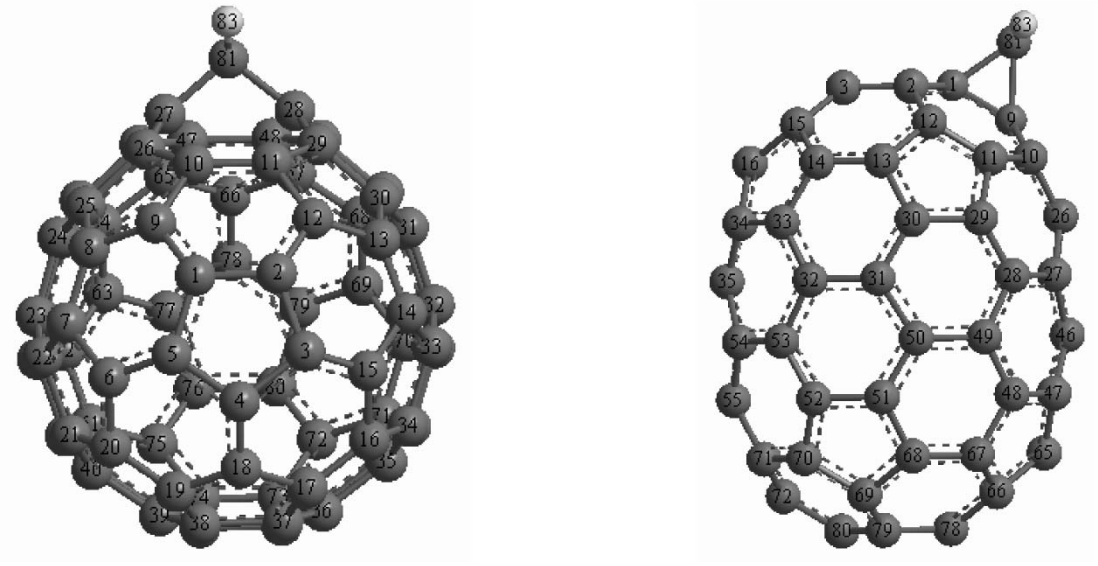

(a) 27,28–$C_{80}CH_2$ with an annulene structure

(b) 1,9–$C_{80}CH_2$ with a cyclopropane structure

Figure 1. The optimized geometries of 27,28–$C_{80}CH_2$ and 1,9–$C_{80}CH_2$ at B3LYP/6-31G level.

1,9–$C_{80}CH_2$(B), where the C(1)–C(9) bond inserted by CH_2 is between the two fused hexagons (6/6 bond) and near the pole of $C_{80}(D_{5d})$. In $C_{80}CH_2$(C), (D) and (E), the C–C bonds added by CH_2 are formed by a hexagon and pentagon (6/5 bonds). In general, the 6/6 bonds in $C_{80}(D_{5d})$ are easier to be added than 6/5 bonds.

The isomers with annulene structures of $C_{80}CH_2$ are more stable than those with cyclopropane structures since the cyclic tension can be reduced in the annulene structures. The lengths of the additive bonds in $C_{80}CH_2$(A), (C), (D), and (E) are 0.2312, 0.2225, 0.2208, and 0.2208 nm, respectively. These bonds are broken, thus the annulene structures are formed. The lengths of the additive bonds in $C_{80}CH_2$(B), (F), and (G) are 0.1633, 0.1658, and 0.1592 nm. These bonds are not opened, thus the cyclopropane structures are formed. The weak additive bonds 0.1468, 0.1473, 0.1462, 0.1457, 0.1435, and 0.1459 nm in $C_{80}CH_2$(A), (C), (D), (E), (H) and (I) lead to the formation of the annulene structures. The strong additive bonds 0.1395, 0.1399, and 0.1404 nm in $C_{80}CH_2$(B), (F), and (G) result in the generation of the cyclopropane structures. The angle of C(27)–C(81)–C(28) in the annulene structure of $C_{80}CH_2$(A) is 101.8°, basically consistent with 111.5° in $C_{80}O$.[10]

In $C_{80}CH_2$(A) with C_s symmetry, the Mulliken atomic charges of the bridged carbon atoms C(27) and C(28) are all 0.0202. The Mulliken charges of C(81), H(82) and H(83) in CH_2 are –0.3816, 0.1703 and 0.1721, respectively, so the bonds C(27)–C(81) and C(28)–C(81) are polar covalent bonds. The Mulliken charge on CH_2 is –0.0392, thus the electrons are attracted from $C_{80}(D_{5d})$ to the CH_2 group.

Electronic absorption spectra: The main absorption peaks in the electronic spectrum of $C_{80}(D_{5d})$ are located at 628.6, 490.6, 423.7, 360.3, 333.2, and 324.9 nm. These absorptions can be comparable to the experimental results of 880, 845, 606, 589, 484, and 446 nm after being multiplied with a factor 1.4. The error is mainly caused by the less configurations used in the calculation and systematic deviation of ZINDO method for higher fullerenes. The strongest peak of $C_{80}(D_{5d})$ appears at 237.3 nm.

Since the absorption at 657.2 nm of $C_{80}(D_{5d})$ arising from HOMO to LUMO is electronically forbidden transition, the first peak at 633.1 nm, the main absorptions at 598.8, 497.6, 371.1, 361.3, 352.0, and the strongest peak at 244.0 nm of $C_{80}CH_2$(A) are red-shifted relative to those of $C_{80}(D_{5d})$ (Figure 2). The first and main absorptions of $C_{80}CH_2$(B) compared with those of $C_{80}CH_2$(A) are blue-

Table 1. Relative energies (E_r) and some parameters (eV) of $C_{80}CH_2$ isomers at B3LYP/6-31G level.

Compounds	E_r	E_{HOMO}	E_{LUMO}	Energy gap	IP	EA	η	χ
27,28–$C_{80}CH_2$(A)	0	–5.1193	–4.0363	1.0830	5.1193	4.0363	0.5415	4.5778
1,9–$C_{80}CH_2$(B)	0.5007	–5.0355	–3.9484	1.0871	5.0355	3.9484	0.5436	4.4920
25,26–$C_{80}CH_2$(C)	0.5551	–5.1220	–3.9811	1.1410	5.1220	3.9811	0.5705	4.5515
1,2–$C_{80}CH_2$(D)	0.5714	–5.0524	–3.9998	1.0525	5.0524	3.9998	0.5263	4.5261
9,10–$C_{80}CH_2$(E)	0.7021	–5.0671	–4.0246	1.0425	5.0671	4.0246	0.5212	4.5458
10,11–$C_{80}CH_2$(F)	0.8680	–4.9582	–4.0167	0.9415	4.9582	4.0167	0.4708	4.4875
26,27–$C_{80}CH_2$(G)	1.0585	–5.1582	–3.8842	1.2740	5.1582	3.8842	0.6370	4.5212
10,26–$C_{80}CH_2$(H)	1.0803	–5.0516	–3.9887	1.0629	5.0516	3.9887	0.5314	4.5201
27,46–$C_{80}CH_2$(I)	1.7252	–5.0660	–4.0390	1.0270	5.0660	4.0390	0.5135	4.5525

Optimized parameters at B3LYP/6-31G level: The energies of HOMO and LUMO of $C_{80}CH_2$(A) are –5.1193 and –4.0363 eV. The energy gap of $C_{80}CH_2$(A) is 1.0830 eV, which is wider than 1.0523 eV of $C_{80}(D_{5d})$. This calculation result is similar to the experiment showing that the electrochemical band gap 1.78 eV of bisadduct of $C_{78}(C_{2v})$ is larger than 1.62 eV of $C_{78}(C_{2v})$.[22] The energy gaps of $C_{80}CH_2$(B), (C) and (D) are 1.0871, 1.1410 and 1.0525, wider than that of $C_{80}(D_{5d})$. As a consequence the stability of $C_{80}CH_2$ to the excitation of electrons will increase.

The IP, EA and χ values of $C_{80}(D_{5d})$ are 5.1667, 4.1144 and 4.6406 eV. The IP, EA and χ values of the $C_{80}CH_2$ isomers are lower than those of $C_{80}(D_{5d})$. Then the $C_{80}CH_2$ isomers readily loose electrons and only with difficulty catch the electrons. Since the η values of $C_{80}CH_2$(A), (B), (C), (D), (G), and (H) are higher than 0.5262 eV of $C_{80}(D_{5d})$, these isomers are thermally more stable.

shifted owing to the wide energy gap. The first and main absorptions of $C_{80}CH_2$(C) and (D) in contrast to those of $C_{80}(D_{5d})$ are red-shifted. When CH_2 is added to $C_{80}(D_{5d})$, the symmetry is reduced, and the peaks split with the decrease in oscillator strength. The more obvious red-shift for the first absorption of $C_{80}CH_2$(I) relative to that of $C_{80}(D_{5d})$ takes place because of the narrow energy gap.

IR spectra: There exist some narrow bands within 500–1000 cm^{-1}, flat region within 1000–1300 cm^{-1} and some strong sharp peaks within 1300–1700 cm^{-1} in the IR spectrum of $C_{80}(D_{5d})$. The main absorptions at 933.4, 1551.2, and 1685.0 cm^{-1} of $C_{80}(D_{5d})$ are ascribed to the puckering vibration of the aryl rings and stretching vibrations of the C–C and C=C bonds. These absorptions split with the decreased intensity in the isomers of $C_{80}CH_2$, which is caused by the addition of the CH_2 group and the decrease in the symmetry.

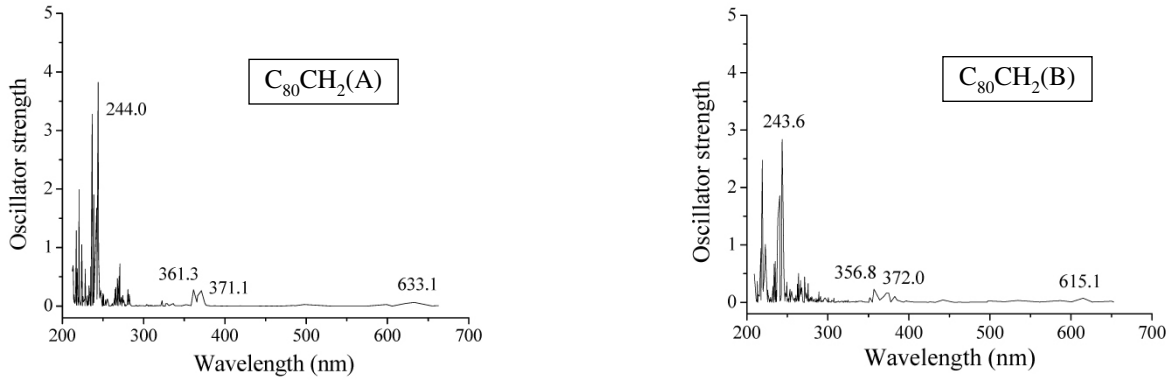

Figure 2. The electronic spectra of $C_{80}CH_2$(A) and (B) using INDO/CIS method.

The strongest peak at 1675.3 cm^{-1} of $C_{80}CH_2$(A) (Figure 3) compared with 1685.0 cm^{-1} of $C_{80}(D_{5d})$ is red-shifted, thus the C=C bonds in $C_{80}CH_2$(A) are weakened. A new absorption at 3153.7 cm^{-1} of $C_{80}CH_2$(A) is produced, which is attributed to the C–H stretching vibration. The main peaks at 1675.3, 1682.4, and 1675.6 cm^{-1} of $C_{80}CH_2$(A), (C), and (I) compared with 1685.0 cm^{-1} of $C_{80}(D_{5d})$ are red-shifted, whereas the absorptions at 1686.6 and 1688.7 cm^{-1} of $C_{80}CH_2$(B) and (F) are blue-shifted. The Mulliken charges of the CH_2 groups in $C_{80}CH_2$(A), (C) and (I) are negative –0.0392, –0.0195, and –0.0068, whereas 0.1918 and 0.1938 of $C_{80}CH_2$(B) and (F) are positive. Since the electrons are attracted from $C_{80}(D_{5d})$ to the CH_2 groups in $C_{80}CH_2$(A), (C), and (I), the electron density on $C_{80}(D_{5d})$ is reduced and the C=C bonds are weakened. On the contrary, the electron density on the cage is increased owing to the positive charges of CH_2 in $C_{80}CH_2$(B) and (F). A similar calculation has shown that the four characteristic bands of $C_{80}O$ compared with those of C_{80} are red-shifted, supporting our conclusion.[10]

Since the electronegativities of the CH_2 groups in the order of $C_{80}CH_2$(A), (C), (I), (B), and (F) are decreasing, the polarities of the C–H bonds are weakened and the covalence characters increased. Thus the strong C–H stretching vibrations at 3153.7, 3163.8, 3168.8, 3174.3, and 3174.6 cm^{-1} in these isomers are gradually intensified.

NMR spectra: The ^{13}C signals of the five unique carbon atoms in $C_{80}(D_{5d})$ are within 124.4–165.4 ppm, which are in agreement with 128.9–163.9 ppm.[1] The lines with the chemical shifts at 152.7 and 165.4 ppm are ascribed to the first and second unique carbon atoms near the pole of $C_{80}(D_{5d})$, which correspond to the experimental values 156.3 and 163.9 ppm.[1] The lines with the chemical shifts at 164.4, 124.4, and 156.5 ppm are assigned as the third, forth, and fifth types of the carbon atoms in $C_{80}(D_{5d})$, and twenty carbon atoms are included in each type.

In $C_{80}CH_2$(A), the signals are distributed within 116.9–174.6 ppm, which arises from the sp^2–C atoms on the cage (Figure 4). This range is wider than that of $C_{80}(D_{5d})$, which is caused by the decrease in symmetry upon the addition of CH_2. The peak at 19.2 ppm of $C_{80}CH_2$(A) arises from the sp^3–C atom in the CH_2 group. The experiment shows that the chemical shifts of the methylene carbon atoms in the isomers of $C_{70}CH_2$ are within 13.8–34.0 ppm.[23] The signals at 179.3 ppm are generated by the bridged carbon atoms C(27) and C(28), which

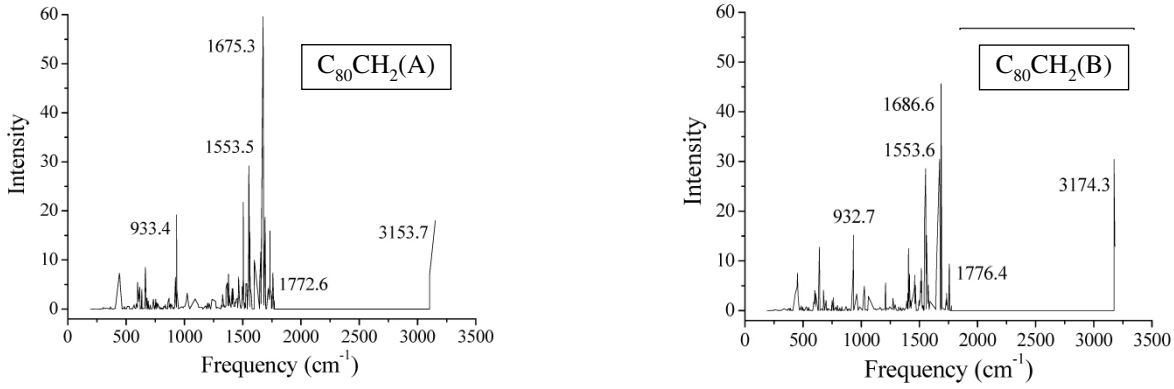

Figure 3. The IR spectra of $C_{80}CH_2$(A) and (B) using PM3 method.

are shifted downfield compared with the value of 156.5 ppm for $C_{80}(D_{5d})$. The electron densities on C(27) and C(28) are lowered owing to the electronegativity of CH_2. In $C_{80}CH_2$(B), the signal at 16.5 ppm is assigned as the sp^3–C atom and the signals of the bridged carbon atoms appear at 78.2 and 92.2 ppm. It has been indicated that the chemical shifts of the bridged carbon atoms in the cyclopropane structure of $C_{60}CH_2$ are 71.0 ppm.[23] At the same time, the region of the chemical shifts for the signals of sp^2–C atoms in $C_{80}CH_2$(B) is changed upfield because of the increased electron density on the cage.

The signals at 19.2, 24.9, and 30.1 ppm of the sp^3–C atoms in the order of $C_{80}CH_2$(A), (C), and (I) are changed downfield because of the decreased electron density. At the same time, the regions of the chemical shifts produced by the sp^2–C atoms in these isomers are changed upfield to 116.9–174.6, 116.0–174.0, and 107.2–172.2 ppm, respectively, because of the increased electron density on the cage. In $C_{80}CH_2$(I), the signals at 107.8 and 107.7 ppm result from the bridged carbon atoms in the annulene structure, which are shifted upfield relative to those of $C_{80}(D_{5d})$ owing to the positive charge on CH_2. These values are similar to 118.0 ppm of the bridged carbon atoms in the annulene isomer of $C_{70}CH_2$.[23]

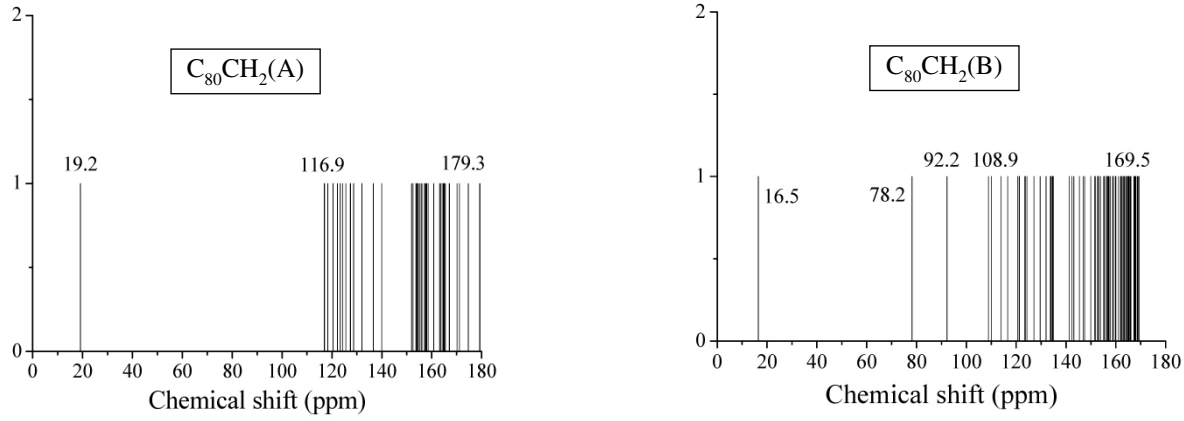

Figure 4. The ^{13}C NMR spectra of $C_{80}CH_2$(A) and (B) at B3LYP/6-31G level.

Aromaticity: The NICS value of $C_{80}(D_{5d})$ at B3LYP/6-31G level was calculated to appear at –8.83 ppm. This method has been successfully used to study the NICS value of $C_{84}(D_2)$.[24] The NICS values of $C_{80}CH_2$(A), (C), (D), (H), and (I) with the annulene structures are located at –7.30, –4.34, –8.73, –7.44, and –6.65 ppm. These values are higher than that of $C_{80}(D_{5d})$ and are similar to the ^{3}He experimental chemical shifts at –27.46 and –27.82 ppm for the two annulene isomers of $C_{70}CH_2$; higher than –28.81 ppm corresponding to $C_{70}(D_{5h})$.[7] The large magnetic cyclic current is maintained in these $C_{80}CH_2$ isomers owing to the formation of the annulene structures. The NICS values of $C_{80}CH_2$(B) and (F) with the cyclopropane structures are situated at –9.85 and –14.63 ppm. These values are lower than that of $C_{80}(D_{5d})$, which is similar to the conclusion that ^{3}He experimental chemical shift at –8.11 ppm for the cyclopropane isomer of $C_{60}CH_2$ is lower than –6.36 ppm of $C_{60}(I_h)$.[7] The magnetic ring current related to π electrons is reduced in $C_{80}CH_2$(B) and (F) because of the transfer of the bridged carbon atoms in the cyclopropane structures from sp^2–C to sp^3–C atoms. Thus the aromaticities of the $C_{80}CH_2$ isomers with the cyclopropane structures relative to that of $C_{80}(D_{5d})$ are predicted to be decreased.

The isomers of $C_{80}CH_2$ with the high NICS values and wide energy gaps such as $C_{80}CH_2$(A) and (C) are more stable than the others, whereas those with the low NICS values and narrow energy gaps like $C_{80}CH_2$(F) are less stable.

4. Conclusions

The most stable isomer at the ground state of $C_{80}CH_2$ was calculated to be 27,28–$C_{80}CH_2$(A) with an annulene-like structure. The first and main absorption peaks in the electronic spectra for the stable $C_{80}CH_2$ isomers relative to those of $C_{80}(D_{5d})$ are red-shifted. The main IR bands of the $C_{80}CH_2$ isomers compared with those of $C_{80}(D_{5d})$ are also red-shifted owing to the negative charges on the CH_2 groups. The ^{13}C chemical shifts of the bridged carbon atoms in $C_{80}CH_2$ with cyclopropane structures are moved upfield upon the formation of the sp^3–C atoms. The bonds near the CH_2 group are activated, becoming the most possible addition sites of the next CH_2 group.

5. References

1. C. R. Wang, T. Sugai, T. Kai, T. Tomiyama, H. Shinohara, *Chem. Commun.* **2000**, 557–558.
2. S.-L. Lee, M.-L. Sun, Z. Slanina, *Int. J. Quantum Chem.: Quantum chemistry Symposium* **1996**, *30*, 1567–1576.

3. Z. Slanina, S.-L. Lee, L. Adamowicz, *Int. J. Quantum Chem.* **1997**, *63*, 529–535.
4. N. B. Shustova, A. A. Popov, M. A. Mackey, C. E. Coumbe, J. P. Phillips, S. Stevenson, S. H. Strauss, O. V. Boltalina, *J. Am. Chem. Soc.* **2007**, *129*, 11676–11677.
5. C. M. Cardona, A. Kitaygorodskiy, A. Ortiz, M. A. Herranz, L. Echegoyen, *J. Org. Chem.* **2005**, *70*, 5092–5097.
6. Y. Iiduka, T. Wakahara, T. Nakahodo, T. Tsuchiya, A. Sakuraba, Y. Maeda, T. Akasaka, K. Yoza, E. Horn, T. Kato, M. T. H. Liu, N. Mizorogi, K. Kobayashi, S. Nagase, *J. Am. Chem. Soc.* **2005**, *127*, 12500–12501.
7. A. B. Smith III, R. M. Strongin, L. Brard, W. J. Romanow, *J. Am. Chem. Soc.* **1994**, *116*, 10831–10832.
8. A. Herrmann, F. Diederich, *J. Chem. Soc. Perkin Trans. 2* **1997**, 1679–1684.
9. J. Škerjanc, *Acta Chim. Slov.* **2006**, *53*, 331–337.
10. M. Ibrahim, *Acta Chim. Slov.* **2005**, *52*, 153–158.
11. H. Sun, Q. Teng, S. Wu, Z. Wang, *Indian J. Chem.* **2006**, *45A*, 1345–1350.
12. M. J. Frisch, G. W. Trucks, H. B. Schlegel, et al., *Gaussian 03, Revision B. 01*, Gaussian Inc., Pittsburgh, PA, **2003**.
13. (a) J. Dolenc, J. Koller, *Acta Chim. Slov.* **2006**, *53*, 229–237. (b) C. Yan, S. Wu, *Acta Chim. Slov.* **2007**, *54*, 755–760.
14. L. Yang, A. M. Ren, J. K. Feng, J. F. Wang, *J. Org. Chem.* **2005**, *70*, 3009–3020.
15. (a) H. Arslan, A. Demircan, *Acta Chim. Slov.* **2007**, *54*, 341–353. (b) A. F. Jalbout, B. Trzaskowski, Y. Xia, Y. Li, *Acta Chim. Slov.* **2007**, *54*, 769–777. (c) R. Abbasoglu, A. Magerramov, *Acta Chim. Slov.* **2007**, *54*, 882–887. (d) W. Zhang, S. Wu, X. Wen, *Indian J. Chem.* **2007**, *46A,* 1911–1916.
16. E. W. Godly, R. Taylor, *Pure Appl. Chem.* **1997**, *69*, 1411–1434.
17. R. D. Bendale, M. C. Zerner, *J. Phys. Chem.* **1995**, *99*, 13830–13833.
18. (a) Q. Teng, S. Wu, *Int. J. Quantum Chem.* **2005**, *104*, 279–285. (b) Q. Teng, S. Wu, *J. Mol. Struct.: Theochem* **2005**, *719*, 47–51. (c) Q. Teng, S. Wu, *J. Mol. Struct.: Theochem* **2005**, *756*, 103–107. (d) S. Wu, Q. Teng, *Int. J. Quantum Chem.* **2006**, *106*, 526–532. (e) Q. Teng, S. Wu, Z. Zhu, *Int. J. Quantum Chem.* **2003**, *91*, 39–45.
19. P. v. R. Schleyer, C. Maerker, A. Dransfeld, H. Jiao, N. J. R. v. E. Hommes, *J. Am. Chem. Soc.* **1996**, *118*, 6317–6318.
20. S. Wu, Q. Teng, *Chinese J. Struct. Chem.* **2005**, *24*, 21–24.
21. K. Nakao, N. Kurita, M. Fujita, *Phys. Rev. B* **1994**, *49*, 11415–11420.
22. C. Boudon, J. P. Gisselbrecht, M. Gross, A. Herrmann, M. Ruttimann, J. Crassous, F. Cardullo, L. Echegoyen, F. Diederich, *J. Am. Chem. Soc.* **1998**, *120*, 7860–7868.
23. A. B. Smith III, R. M. Strongin, L. Brard, G. T. Furst, W. J. Romanow, K. G. Owens, R. J. Goldschmidt, R. C. King, *J. Am. Chem. Soc.* **1995**, *117*, 5492–5502.
24. H. Sun, S. Wu, X. Ren, *J. Mol. Struct.: Theochem* **2008**, *855,* 6–12.

Povzetek

S pomočjo teorije gostotnih funkcionalov (DFT) na nivoju B3LYP/6-31G smo preučili elektronsko strukturo in stabilnost devetih možnih izomerov $C_{80}CH_2$, ki temeljijo na strukturi $C_{80}(D_{5d})$. Glede na optimizirane geometrije smo z metodami INDO/CIS, PM3 in B3LYP/6-31G izračunali elektronske, IR in ^{13}C NMR spektre izomerov $C_{80}CH_2$. Kot najbolj stabilno geometrijsko obliko $C_{80}CH_2$ smo napovedali 27,28–$C_{80}CH_2$(A) z anulensko strukturo, kjer je adicija potekla na vez 6/6 blizu ekvatorialnega pasu molekule $C_{80}(D_{5d})$. Položaj prve absorpcijske črte v elektronskih spektrih in območje glavnih absorpcij v IR spektrih so za $C_{80}CH_2$ v primerjavi z $C_{80}(D_{5d})$ pomaknjeni bolj v rdeče območje. Kemijski premiki v ^{13}C NMR spektrih so za mostne atome v ciklopropanski strukturi glede na premike v anulenski strukturi premaknjeni v višje polje. Aromatičnost je večja v anulenski kot v ciklopropanski strukturi, kar je skladno z NICS vrednostmi za $C_{80}CH_2$ napovedanimi na nivoju B3LYP/6-31G.

Supporting materials:

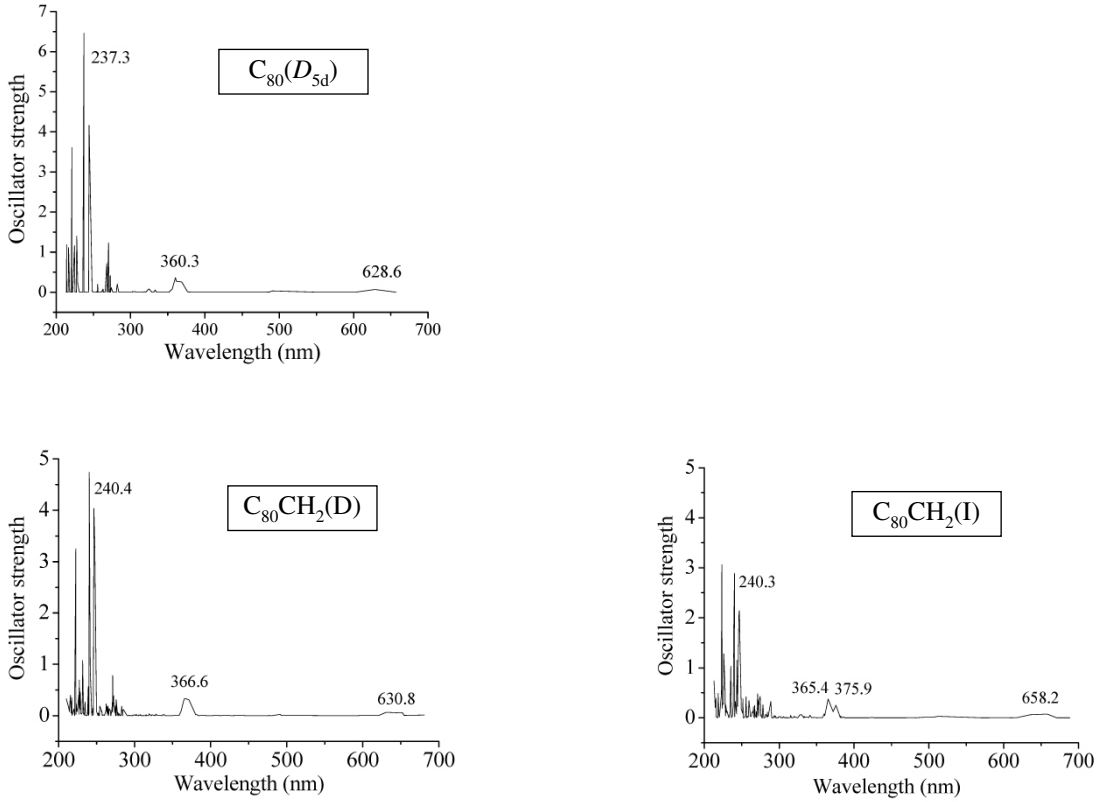

Figure 1. The electronic spectra of $C_{80}(D_{5d})$, $C_{80}CH_2$(D) and (I) using INDO/CIS method.

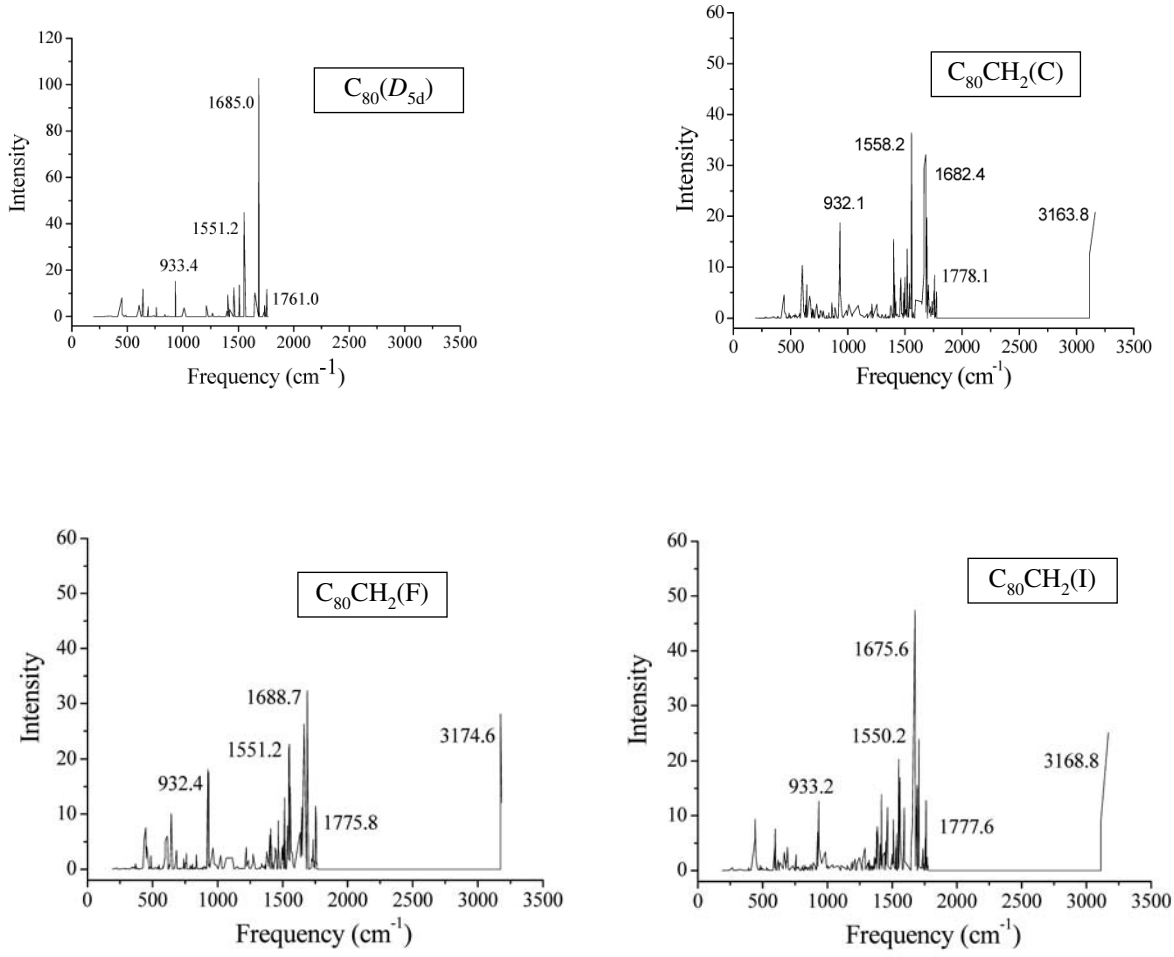

Figure 2. The IR spectra of $C_{80}(D_{5d})$, $C_{80}CH_2$(C), (F), and (I) using PM3 method.

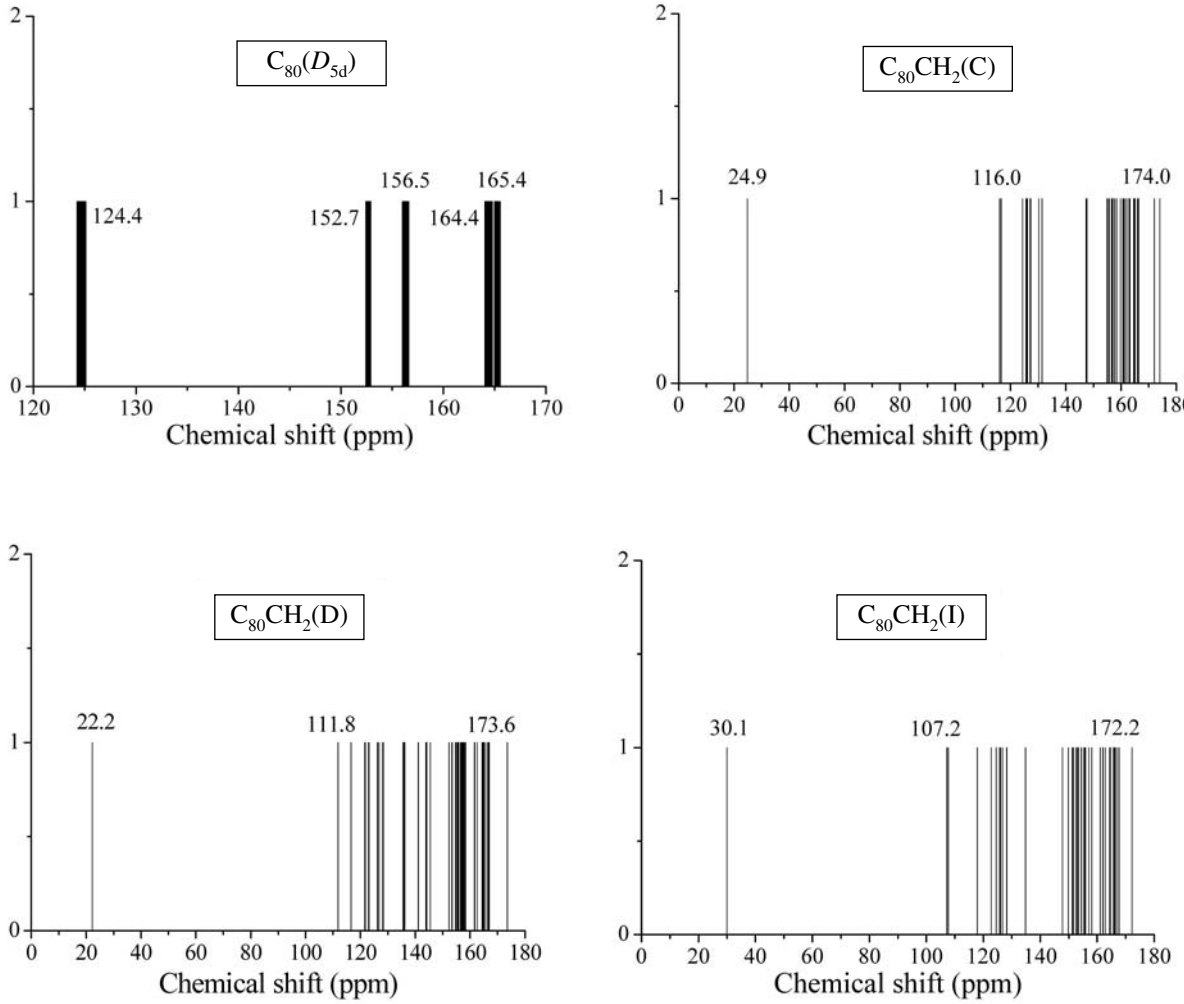

Figure 3. The ^{13}C NMR spectra of $C_{80}(D_{5d})$, $C_{80}CH_2$(C), (D), and (I) at B3LYP/6-31G level.